By the nature of the Levins-type metapopulation used here, all epidemiological dynamics within a subpopulation are ignored. This means that as soon as a township is infected it can transmit infection as strongly as when endemic equilibrium has been reached. In an ideal situation, the within-subpopulation dynamics should also be included and modeled stochastically. However, the Levins approximation allows for very rapid computation and therefore far richer parameterization; it also circumvents the difficulty of estimating the racoon population levels within each township. This is a good example of where limitations of the available data determine the appropriate model choice, and where simple models can be used to derive the main conclusion that rivers act as significant but permeable barriers to the spread of rabies in racoons.

7.3. LATTICE-BASED MODELS

There are many occasions when the spatial location of the hosts is seen to be important, but there is no natural means of partitioning the entire population into discrete subpopulations. In such situations, lattice- or grid-based models are often used, where individuals within a grid site are grouped together into a subpopulation. Traditionally, these grid-based models take two forms: coupled lattice models that can be considered as a grid of subpopulations with coupling between adjacent grid sites (neighbors), and cellular automata where at most one host can occupy each grid site and again interactions occur only locally with the neighboring sites. In essence, both of these models are special forms of the metapopulation model, with a tightly constrained set of interactions. In general, these models are conceptual tools, used to inform about the effects of spatial separation and nonrandom mixing; they are seldom used as accurate predictive tools, because with few exception (such as orchards) most hosts do not exist on regular lattices. However, the insights provided by this type of model have proved to be invaluable in understanding the spatial spread of infection (White and Harris 1995; Tischendorf et al. 1998; Keeling and Gilligan 2000; Rushton et al. 2000; Kao 2003).

Two main types of lattice exist, which determine how the entire population is divided into subpopulations. Probably the most intuitive is the two-dimension square lattice, so that an individual's position (on the surface of the earth) is translated into x and y coordinates which in turn determine the grid site (White and Harris 1995). Modifications to this standard grid arise by changing the number of dimensions; many theoretical problems can be studied more precisely if the populations are arranged along a one-dimensional line, with interactions between nearest (or nearest and next-nearest) neighbors (Harris 1974; Watts and Strogatz 1998). Alternatively, higher dimensional lattices can also be used to replicate the more complex higher-dimensional social structure of humans (Rhodes et al. 1997). Square lattices impose a definite direction on the space (mathematically we lose the property of isotropy) such that the directions "north," "south," "east," and "west" play a more major role than any others. To overcome this problem, some researchers have used hexagonal grids, where each site has six neighbors; this often generates more natural spatial patterns (van Baalen and Rand 1998; Kao 2003).

7.3.1. Coupled Lattice Models

Although coupled lattice models are simply a special case of the metapopulation formulation, it will be worth considering some of the particular differences in more detail. For

a disease with SIR-type dynamics and "commuter-like" interaction terms (see Section 7.2.1), the governing equations become:

This is online program 7.3

$$\begin{aligned}
\frac{dX_i}{dt} &= \mu - \beta X_i \frac{(1-\sum_j \rho_{ji})Y_i + \sum_j \rho_{ij} Y_j}{(1-\sum_j \rho_{ji})N_i + \sum_j \rho_{ij} N_j} - \nu X_i, \\
\frac{dY_i}{dt} &= \beta X_i \frac{(1-\sum_j \rho_{ji})Y_i + \sum_j \rho_{ij} Y_j}{(1-\sum_j \rho_{ji})N_i + \sum_j \rho_{ij} N_j} - \gamma Y_i - \nu Y_i, \qquad (7.16) \\
\rho_{ij} &= \rho_{ji} = \begin{cases} \rho & \text{if } i \text{ and } j \text{ are neighbors} \\ 0 & \text{otherwise,} \end{cases}
\end{aligned}$$

where i refers to a grid cell within the lattice. (Given that lattices are usually two-dimensional, some researchers prefer to specify a subpopulation by its coordinates; therefore, X_{ij} is the number of susceptibles at location (i, j). However, this notation can be very cumbersome when we wish to specify the level of interaction between two locations (e.g., $\rho_{(i,j)(k,l)}$)).

Equation (7.16) assumes that all populations have identical demographic and epidemiological parameters, and therefore we have moved further away from data-driven models such as those illustrated in Section 7.2.1.3. However, this assumption of homogeneity of parameters allows for a more detailed understanding of the spatio-temporal dynamics. In addition, it is frequently assumed that all populations are of equal size ($N_i = N$), which simplifies the denominator in equation (7.16) to N.

Coupled lattice models are specialized metapopulation models, where subpopulations are arranged on a grid and coupling is generally to the nearest neighbors only.

The most notable feature of this form of lattice model is the clear wave-like spread of invading infections. From a point source of infection, the disease must spread to the neighboring sites before it can spread to the rest of population. Figure 7.9 shows a pictorial example of the wave-like spread for a square lattice, together with a graph of how coupling (ρ) and the basic reproductive ratio ($R_0 = \frac{\beta}{\gamma+\nu}$) both determine the speed of the invading wave.

As with the metapopulation models, a stochastic version of the lattice model has a slower wave speed than the deterministic model, and when the deterministic wave speed is very low the stochastically spreading disease may even fail to colonize the entire lattice. This reduction in speed is because in an integer-based stochastic model transmission of infection into a new subpopulation is a stochastic process and therefore may, by chance, be considerably delayed; by contrast, in a deterministic model very low prevalence will always spread to the new subpopulations. As expected, increasing the level of interaction between neighboring subpopulations, or increasing the within-subpopulation growth rate, allows the infection to spread more rapidly.

The wave speed of an invading epidemic in a coupled-lattice model increases almost linearly with the initial growth rate of the infection, $\beta - \gamma - \nu$; increases nonlinearly with the level of coupling, ρ; and is slightly more rapid in deterministic compared to stochastic models.

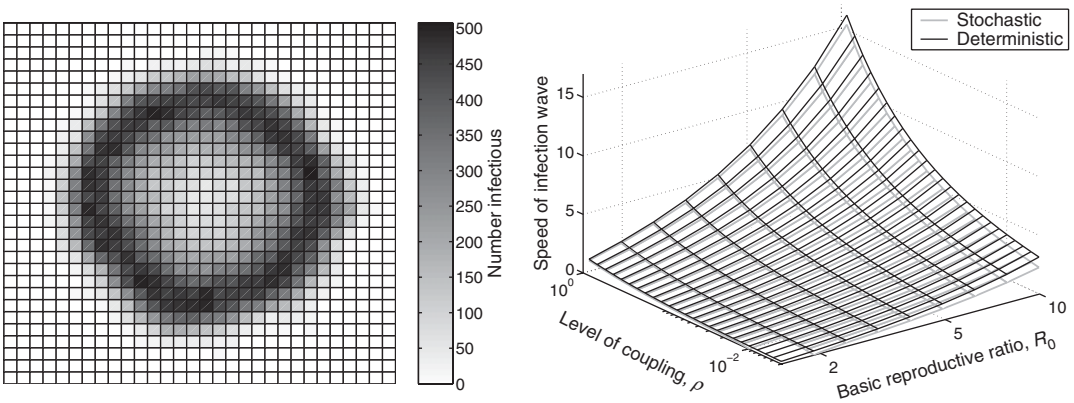

Figure 7.9. Results from a coupled lattice model using the approximate commuter-type coupling (equation (7.16)). The left-hand figure shows a snapshot of the lattice at time $t = 5$, with darker shades illustrating a higher level of infectious individuals ($R_0 = 5$, $\rho = 0.1$). The circular wavelike spread of infection is clear. The right-hand graph shows the speed of the invading wave of infection as the basic reproductive ratio and the level of coupling vary. The model simulates the spread of infection on a 100×100 lattice; the local subpopulations are all identical and contain 1,000 individuals. ($\gamma = 1$; changing this would scale the speed of the invading wave).

In contrast to metapopulations where space is often rather abstract, coupled lattice models provide a definite method of including the spatial location of individuals. This allows us to predict the expected wavelike spread of infection across a homogeneous spatial landscape. As such, coupled lattice models play a vital role in improving our understanding of the spatial spread of infection; they can be readily derived from the standard nonspatial models, and due to the simplistic assumptions about spatial interaction require very little extra information to parameterize. However, such coupled lattice models break down if we attempt to match them too rigorously to the underlying individual-level spatial dynamics. This difficulty arises because of the assumption that mixing within a grid site is completely random (and full strength), whereas mixing between adjacent cells is far weaker. Figure 7.10 shows an example of how the coupled-lattice assumption can fail to capture the expected individual-level behavior. Because individuals A and B are within the same grid cell, the coupled lattice assumption means that the interaction between them is strong, whereas the interaction between B and C (and A and D) is far weaker or zero because they lie in separate cells despite the fact that the separations involved are smaller. This highlights a fundamental flaw with coupled lattice models: The act of artificially aggregating populations into grids can lead to some artificial results and hence the grid size must be chosen with extreme care.

7.3.2. Cellular Automata

Cellular automata also use a lattice-based arrangement of sites. However, in contrast to the lattice-based models discussed above, cellular automata have only a finite, and usually small, number of population states. Most frequently we consider each lattice site to represent a single host (a population size of one) and so each site is generally either empty,

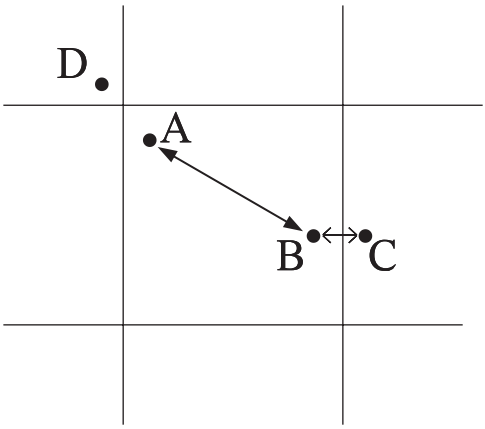

Figure 7.10. A representation of when the coupled-lattice framework may fail to describe the expected interaction between individuals. Although A and D and (B and C) are close, the interaction between them is weak because they occupy different grid locations.

or occupied by a susceptible, infectious, or recovered individual. Due to this finite nature almost all cellular automata disease models are stochastic.

Cellular automata are clearly an abstraction of reality. Other than in agricultural settings (Maddison et al. 1996; Klecakowski et al. 1997; Gibson 1997b), individuals do not often exist in fixed lattice arrangements. In addition, the small number of interaction neighbors that are usually assumed (just the nearest 4 or 8 lattice sites) are unrepresentative of the complex and heterogeneous contacts through which human and animal infections pass. However, cellular automata are superb tools to understand how the individual and spatial nature of populations causes epidemic dynamics to deviate from their deterministic random-mixing ideal.

Cellular automata operate on a lattice of sites, with each site generally assumed to hold a single host. Interaction is usually stochastic and with the neighboring (4 or 8) lattice sites.

Two basic forms of cellular automata dominate the early literature in this subject area, and have clear parallels to disease models. These are the contact process, which is equivalent to the SIS model, and the forest-fire model, which is equivalent to an SIR-type infection.

7.3.2.1. The Contact Process

The contact process, which dates back to 1974, is traditionally formulated in one dimension so that individuals are positioned in a row with contact between adjacent individuals (Harris 1974). The stochastic rules that govern the behavior of this model, when translated into a disease metaphor are biologically intuitive. Infectious individuals transmit infection at a rate τ to any neighboring susceptible and infectious individuals recover at a rate γ, becoming susceptible to the disease once more—this is clearly the SIS model (Chapter 2) in a spatial context. By considering a central individual and both neighbors, we can

explicitly define the possible rates of change:

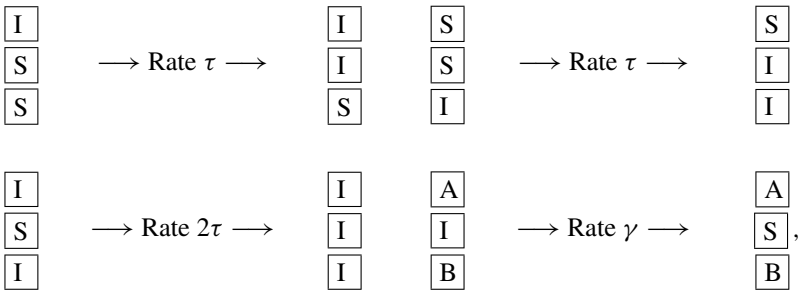

where A and B can be either S or I.

For this contact process we want to calculate R_0, thereby linking the individual level parameters τ and γ to population-level dynamics. If we consider R_0 as the rate that secondary cases are initially produced, multiplied by the infectious period (Chapter 2), then it is clear that $R_0 = 2\frac{\tau}{\gamma}$, where 2 comes from the fact that every individual has 2 contacts. This would suggest that the disease can invade and expand throughout the population if $\tau > \frac{1}{2}\gamma$. However, such arguments do not take into account the spatial structure that develops during the early epidemic process. Consider the initial seed infection, where by chance it infects a neighboring contact; however, this neighbor now has only one susceptible neighbor (unless the seed infection recovers) and therefore has a much reduced potential for spreading the infection. We therefore observe a common phenomenon in many spatial disease models: The local pool of susceptibles is rapidly depleted, which can dramatically reduce the early growth rate.

In many spatial models, the depletion of the locally available susceptible population can reduce the early growth rate of the epidemic and the speed of the invading wave front.

Even for this most simple of individual-based spatial models, the precise threshold value of τ that allows an epidemic to spread can be calculated only by repeated large-scale numerical simulation. The latest estimates suggest that $\tau > 1.64896\gamma$ for the infection to have a nonzero probability of long-term spread and persistence (de Mendonça 1999).

7.3.2.2. The Forest-Fire Model

A second common form of cellular automata is the forest-fire model, which is closely associated with spread of $SIRS$-type infection and is usually simulated on a two-dimensional lattice. In the original notation, lattice sites can be empty, occupied by a healthy tree, or occupied by a burning tree. Burning trees die to leave empty spaces, fire can spread between neighboring trees, trees can colonize empty spaces, and occasional random lightning strikes can cause spontaneous fires. In epidemiological notation, healthy trees are susceptibles, burning trees are infectious, empty sites are recovered (and immune), colonization by trees mimics either the birth of new susceptibles or waning immunity, and lightning represents the import of infection. Again we describe the dynamics in terms of

the rates of change of lattice sites:

$$\boxed{S} \longrightarrow \boxed{I} \quad \text{Rate} = \tau n + \varepsilon \text{ where } n \text{ is the number of infectious neighbors.}$$

$$\boxed{I} \longrightarrow \boxed{R} \quad \text{Rate} = \gamma.$$

$$\boxed{R} \longrightarrow \boxed{S} \quad \text{Rate} = \nu.$$

This is online program 7.4

This model was developed by Per Bak and coworkers (Bak et al. 1990), and for statistical physicists displays a range of interesting power-law scaling and self-organized critical behavior. In general, distributions such as the size of patches of susceptibles (trees) or the size of individual epidemics are observed to follow a power-law relationship (frequency $\propto$ size$^{-\alpha}$), with the power-law exponent, α, being largely independent of the precise parameter values. This behavior occurs whenever certain rates of change are much bigger than others; in particular, transmission is much faster than recovery, which is much faster than births, which is much faster than random imports of infection ($\tau \gg \gamma \gg \nu \gg \varepsilon$). Fortunately, this natural ordering holds in most epidemiological examples, so it is hoped that the same power-law scaling and ideas of self-organized criticality will hold also. Much more information on self-organized criticality can be found in the following publications: Tang and Bak (1988); Sole et al. (1999); Allen et al. (2001); Pascual and Guichard (2005).

The forest-fire model typifies many stochastic spatial models. The fact that transmission is faster than recovery, which is faster than births, which is faster than imports of infection, leads to power-law relationships between epidemic size and frequency.

7.3.2.3. Application: Power-Laws in Childhood Epidemic Data

The work of Rhodes and coworkers (Rhodes and Anderson 1997; Rhodes et al. 1997) provides a good example of how cellular automata models can be used to develop deeper insights into the roles of spatial structure and individual-based populations in the dynamics of infectious diseases. They were interested in the dynamics of childhood diseases, and the distribution of outbreak sizes in small isolated populations. The Fareo Islands are isolated islands in the North Atlantic between Scotland and Iceland, and have a population of around 25,000. These island have extremely good historical records of infectious disease outbreaks stretching back for around 100 years (Cliff et al. 1993), and so are an ideal source of data for epidemiological study. In a number of papers, Rhodes and coworkers showed that the outbreaks of childhood diseases in the Faroes follow a power-law relationship, and that a similar scaling can be obtained from a biologically simple cellular automaton model.

In Figure 7.11, we show how the frequency of epidemics greater than or equal to a given size decreases, following a power-law like relationship. For epidemics of fewer than 500 cases, the probability that the epidemic is greater than or equal to size s is given by:

$$\mathbb{P}(\text{epidemic} \geq s) = s^{-\alpha},$$

with $\alpha \approx 0.265$ for measles, $\alpha \approx 0.255$ for whooping cough, and $\alpha \approx 0.447$ for mumps. This is reminiscent of the power-law relationships that are seen in the traditional

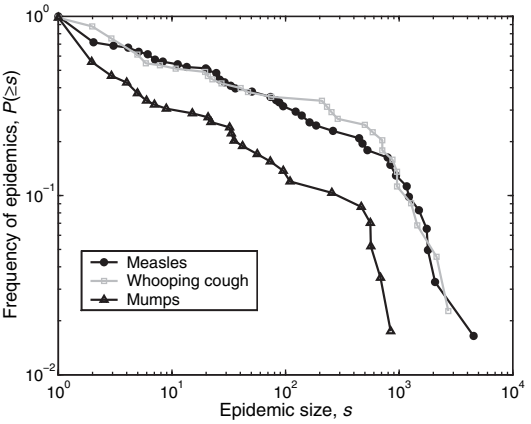

Figure 7.11. The power-law scalings observed in the epidemic outbreak data from the Faroe Islands, 1870–1970. The frequency of epidemics greater than or equal to a given size is shown for three major childhood infections: measles, whooping cough (pertussis), and mumps. It is postulated that a power-law scaling holds for epidemics up to 500–1,000 cases. The graph is plotted on a log-log scale, so that straight lines equate to power-laws. (From Rhodes et al. 1997.)

forest-fire model; therefore, Rhodes and Anderson modified the standard model to overcome some of the limitations and incorporate more realistic human behavior. In particular, the susceptible and infectious hosts are no longer fixed but are able to wander across the lattice by moving into neighbored unoccupied cells. This movement of individuals means that the behavior of adjacent sites is related (because the movement from one cell must be balanced by the movement *to* another), breaking the independence assumptions of formal cellular automata. However, the same basic techniques and results still translate between true cellular automata and this more complex model.

Figure 7.12 shows examples of the Rhodes and Anderson model in two and three dimensions. In two dimensions, the lattice is a 158×158 square, and each site has four nearest neighbors involved in the transmission of infection and movement; in three-dimensions, the lattice is a $29 \times 29 \times 29$ cube, and each site has six neighbors. Although the power-law distribution of (relatively) small epidemic sizes is largely independent of the precise parameter values, the behavior does vary with the dimension of the system. In three dimensions, the distribution of epidemic sizes is a much closer fit to a power-law of $\alpha \approx 0.2$ than when the model is two-dimensional, and therefore seems a plausible representation of measles or whooping cough. When the lattice is made five-dimensional, the power-law changes to $\alpha \approx 0.4$ (Rhodes et al. 1997), and therefore is comparable with the scaling exponent observed for mumps.

It is important to ask what these theoretical results mean at a practical level. Rather that telling us that models in three and five dimensions are required to capture the behavior of measles, whooping cough, and mumps, these results indicate that simple nearest-neighbor transmission in two dimensions is insufficient to describe the true nature of human social contacts. Three and five dimensions are simply methods of introducing the added elements of complexity, clustering, and interaction that exist in human social networks. This reinforces our original contention that most lattice models are abstract tools that can be used to improve our understanding of transmission in a spatial environment, rather than detailed predictive models.